

## Geology

### A low-velocity zone with weak reflectivity along the Nankai subduction zone

Jin-Oh Park, Gou Fujie, Lalith Wijerathne, Takane Hori, Shuichi Kodaira, Yoshio Fukao, Gregory F. Moore, Nathan L. Bangs, Shin'ichi Kuramoto and Asahiko Taira

*Geology* 2010;38;283-286  
doi: 10.1130/G30205.1

---

**Email alerting services** click [www.gsapubs.org/cgi/alerts](http://www.gsapubs.org/cgi/alerts) to receive free e-mail alerts when new articles cite this article

**Subscribe** click [www.gsapubs.org/subscriptions/](http://www.gsapubs.org/subscriptions/) to subscribe to *Geology*

**Permission request** click <http://www.geosociety.org/pubs/copyrt.htm#gsa> to contact GSA

Copyright not claimed on content prepared wholly by U.S. government employees within scope of their employment. Individual scientists are hereby granted permission, without fees or further requests to GSA, to use a single figure, a single table, and/or a brief paragraph of text in subsequent works and to make unlimited copies of items in GSA's journals for noncommercial use in classrooms to further education and science. This file may not be posted to any Web site, but authors may post the abstracts only of their articles on their own or their organization's Web site providing the posting includes a reference to the article's full citation. GSA provides this and other forums for the presentation of diverse opinions and positions by scientists worldwide, regardless of their race, citizenship, gender, religion, or political viewpoint. Opinions presented in this publication do not reflect official positions of the Society.

---

#### Notes

# A low-velocity zone with weak reflectivity along the Nankai subduction zone

Jin-Oh Park<sup>1,2\*</sup>, Gou Fujie<sup>2</sup>, Lalith Wijerathne<sup>2</sup>, Takane Hori<sup>2</sup>, Shuichi Kodaira<sup>2</sup>, Yoshio Fukao<sup>2</sup>, Gregory F. Moore<sup>2,3</sup>, Nathan L. Bangs<sup>4</sup>, Shin'ichi Kuramoto<sup>5</sup>, and Asahiko Taira<sup>5</sup>

<sup>1</sup>Ocean Research Institute, University of Tokyo, Tokyo 164-8639, Japan

<sup>2</sup>Institute for Research on Earth Evolution, Japan Agency for Marine-Earth Science and Technology, Yokohama 236-0001, Japan

<sup>3</sup>Department of Geology and Geophysics, University of Hawaii, Honolulu, Hawaii 96822, USA

<sup>4</sup>Institute for Geophysics, University of Texas, Austin, Texas 78758-4445, USA

<sup>5</sup>Center for Deep Earth Exploration, Japan Agency for Marine-Earth Science and Technology, Yokohama 236-0001, Japan

## ABSTRACT

Three-dimensional seismic reflection data reveal the presence of a low seismic velocity zone (LVZ) with weak reflectivity character along the Nankai accretionary prism. This LVZ is intercalated between an upper, offscraped layer and a lower, underthrusting layer in the outer accretionary wedge. Wide-angle ocean bottom seismograph data also support the presence of the LVZ, which is estimated to be a maximum of ~2 km thick, ~15 km wide, and ~120 km long. The LVZ could be an underthrust package underplated in response to the lateral growth of the Nankai accretionary prism. Underplating of the underthrusting layer beneath the overlying offscraped layer would maintain a critical taper of the accretionary prism so that the offscraped layer can continue to grow seaward. The LVZ could have elevated fluid pressure, leading to rigidity reduction of the entire outer accretionary wedge. The rigidity-lowered outer wedge, containing the LVZ, may be more easily uplifted and thus eventually foster tsunami generation during a Nankai megathrust earthquake. If the fluid-rich LVZ supplies a significant amount of the fluid to the megasplay fault zone at depth, it may affect stick-slip behavior of the fault.

## INTRODUCTION

The existence of low seismic velocity zones along the plate interface has been reported at various convergent margins around the world, e.g., Alaska (Moore et al., 1991), Costa Rica (Christeson et al., 1999), Cascadia (Nedimovic et al., 2003), Ecuador (Sage et al., 2006), and Chile (Groß et al., 2008). Most of these studies focused on the formation of a subduction channel and/or fluid flow along the plate boundary, except for the Alaska margin. Previous studies of detailed crustal structure and the lateral extent of the low-velocity zone (LVZ) along the trench have been limited to interpretations of structures observed by two-dimensional (2-D) seismic reflection or wide-angle ocean-bottom seismograph (OBS) data.

The Nankai Trough subduction zone off southwest Japan is one of the convergent margins best suited for studying large megathrust earthquakes, as well as the formation of accretionary prisms. In particular, the Nankai subduction zone off Kii Peninsula (Fig. 1) is characterized by a steeply landward-dipping megasplay fault (Park et al., 2002; Moore et al., 2007) in the rupture area of the 1944 Tonankai earthquake (M 8.1). This megasplay fault branches upward from the plate interface (i.e., the megathrust fault), breaking through the overlying accretionary wedge.

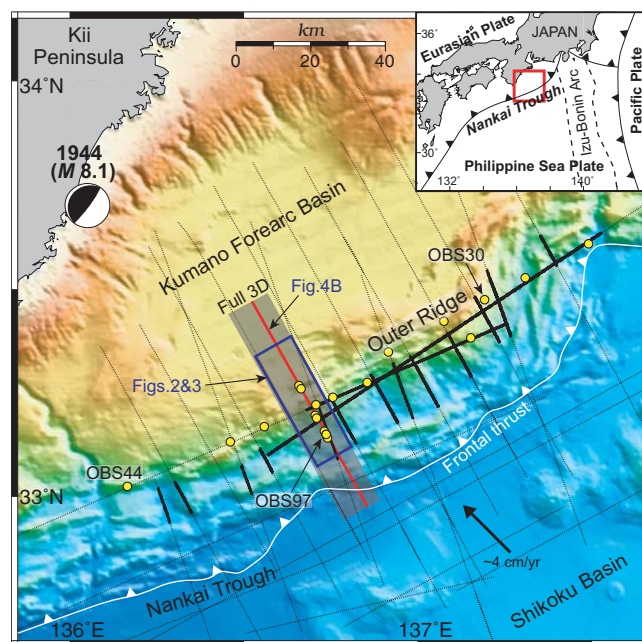
A few 2-D seismic reflection surveys have been conducted to determine the overall crustal

structure off Kii Peninsula (Park et al., 2002, 2003). However, structural details needed to interpret the upper plate, including the overlying accretionary wedge, are too complex to image well with 2-D seismic imaging. In 2006 we carried out a three-dimensional (3-D) multi-

channel seismic (MCS) reflection survey across the Nankai Trough off the southeast Kii Peninsula (Fig. 1) to resolve the detailed structure of the subduction zone. We acquired the 3-D MCS data over a 12 km × 62 km area intended to include most of the drilling sites of the Integrated Ocean Drilling Program (IODP) project Nankai Trough Seismogenic Zone Experiment (NanTroSEIZE). For detailed seismic reflection imaging and estimating *P*-wave interval velocity (*V<sub>p</sub>*), important for quantifying the physical properties below the seafloor, we have carried out 3-D prestack depth migration (PSDM) processing using the 3-D MCS data. The 3-D PSDM results have revealed an LVZ with weak reflectivity character along the Nankai subduction zone. Several OBS records helped to constrain the lateral extent of the LVZ.

In this paper we document the presence of the LVZ, and propose a tectonic model associating LVZ formation with the underplating process.

**Figure 1. Seafloor bathymetry and locations of two-dimensional (2-D) multichannel seismic (MCS) reflection lines (thin black dotted) and 3-D (shaded in gray) in Nankai Trough margin off southwest Japan. Inset: Regional map showing location of study area (red box). A blue box (11 km × 34 km) within the full 3-D survey area (12 km × 62 km) is shown in Figures 2 (see footnote 1) and 3. A 3-D prestack depth migration (PSDM) velocity model of line in red is shown in Figure 4B (see footnote 1). Low-velocity zone (LVZ) with weak reflectivity character is identified over 3-D survey area between outer ridge and frontal thrust. Black thick portions of the 2-D lines represent a sedimentary unit of weak reflectivity, inferred to be LVZ. Yellow circles are wide-angle ocean-bottom seismographs (OBSs) showing a shadow zone, supporting presence of LVZ. Observed wide-angle seismic data from OBS97, OBS30, and OBS44 are shown in Figures 4A, 4C, and 4D, respectively.**



\*E-mail: [jopark@ori.u-tokyo.ac.jp](mailto:jopark@ori.u-tokyo.ac.jp).

Finally, we present potential implications of the LVZ for tsunami generation and megasplay fault behavior.

## GEOLOGIC SETTING AND BACKGROUND

At the Nankai Trough margin, the Philippine Sea plate is being subducted beneath the Eurasian plate to the northwest at a convergence rate of ~4 cm/yr (Seno et al., 1993). The Shikoku Basin, the northern part of the Philippine Sea plate, is estimated to have opened between 25 and 15 Ma ago by backarc spreading of the Izu-Bonin arc (Okino et al., 1994). Late-stage reorientations of spreading in Shikoku Basin caused large variations in basement relief. Some of the seafloor bathymetric features, such as ridges or seamounts, are subducting beneath the Nankai accretionary wedge (e.g., Park et al., 1999, 2003), causing deformation of the wedge.

The >100-km-wide Nankai accretionary wedge, which has developed landward of the trench since the Miocene, mainly consists of offscraped and underplated materials from the trough-fill turbidites and the Shikoku Basin hemipelagic sediments. The basic processes of the accretion are considered to be lateral and vertical growth through offscraping and underplating (Moore and Silver, 1987). Underplating has been reported in the ancient accretionary prism of the Cretaceous–Tertiary Shimanto Belt, which is widely exposed in southwest Japan (e.g., Kimura and Mukai, 1991). The critical taper of the Nankai accretionary prism tends to increase from west to east (Kimura et al., 2007). A trench sediment wedge ~1.3 km thick overlies ~1.1 km of Shikoku Basin hemipelagic sediment in the 3-D survey area, where all of the trench sediment and at least half of the Shikoku Basin sediment are accreted to form a wide accretionary prism (Park et al., 2002).

Historic, great megathrust earthquakes with a recurrence interval of 100–200 yr (e.g., Ando, 1975) have generated large tsunamis along the Nankai Trough margin. The A.D. 1605 Keicho ( $M$  7.9) event is particularly well known as a tsunami earthquake that affected coastal areas around the Nankai subduction zone (Ishibashi, 1983).

## SEISMIC DATA AND INTERPRETATION

### 3-D Seismic Reflection Data and Interpretation

Final 3-D PSDM results, both the seismic reflection image and the  $V_p$  model of the Nankai accretionary wedge, are shown in Figure 2<sup>1</sup> (for details of the 3-D data acquisition and processing, see the caption of Fig. 2). The final 3-D

PSDM clearly images detailed crustal structures. However, due to the length of the streamers (4500 m) and the strong feathering, uncertainty in velocities and depth inferred from the 3-D PSDM at depths greater than the streamer length are unavoidable. In order to verify the accuracy of the PSDM velocity model, we performed an uncertainty test using the migration velocity scan analysis to check the flatness of the PSDM gather reflections for various velocity ranges. Consequently, the velocity model showed a maximum of 10% uncertainty at ~6 km depth.

On the basis of on reflection characteristics and  $V_p$ , we identify three major seismic reflection units in the accretionary prism outer wedge between the outer ridge and the seaward frontal thrust (Fig. 3): from top to bottom, these are unit A, unit B, and unit C. Unit A has a  $V_p$  of 1.6–3.5 km/s and is characterized by many folds and imbricate thrust faults. Unit A is highly reflective, and we interpret it to be formed of mainly offscraped and accreted trench-fill turbidite sediment, commonly observed in the Nankai accretionary wedge system (Moore et al., 1990). Unit B, just above the strong amplitude décollement reflection, shows a  $V_p$  of 2.7–3.2 km/s and weak reflectivity. Even though there is a velocity reversal with depth between units A and B, we do not observe a negative polarity at

the base of unit A. Unit C, between the décollement reflection and top of oceanic crust, shows a  $V_p$  of 3.5–4.0 km/s and is almost transparent or has weak reflectivity. We interpret unit C to be a layer of underthrust Shikoku Basin hemipelagic sediment, also commonly observed in the Nankai accretionary wedge system. The positive polarity of the décollement reflection is consistent with the positive velocity contrast with depth between units B and C.

The weak reflectivity LVZ (unit B) has not previously been recognized in any 2-D or 3-D MCS data over the Nankai accretionary wedge. The LVZ that is intercalated between an upper, fold-and-thrust offscraped layer (unit A) and a lower, underthrust layer (unit C), is ~0.5–2.0 km thick, and tends to thin seaward. The landward extent of the LVZ beyond the outer ridge is not obvious. Considering the maximum of 10% velocity uncertainty at ~6 km depth that almost corresponds to the base of unit A, the velocity reversal of ~0.8 km/s between units A and B is quite significant, supporting the presence of the LVZ.

The LVZ along the shallow Nankai subduction zone exhibits a weak reflectivity, while other LVZs along deeper subduction zones show strong or high reflectivity. For example, in the Cascadia margin (Nedimovic et al., 2003), an LVZ with high reflectivity is interpreted to be

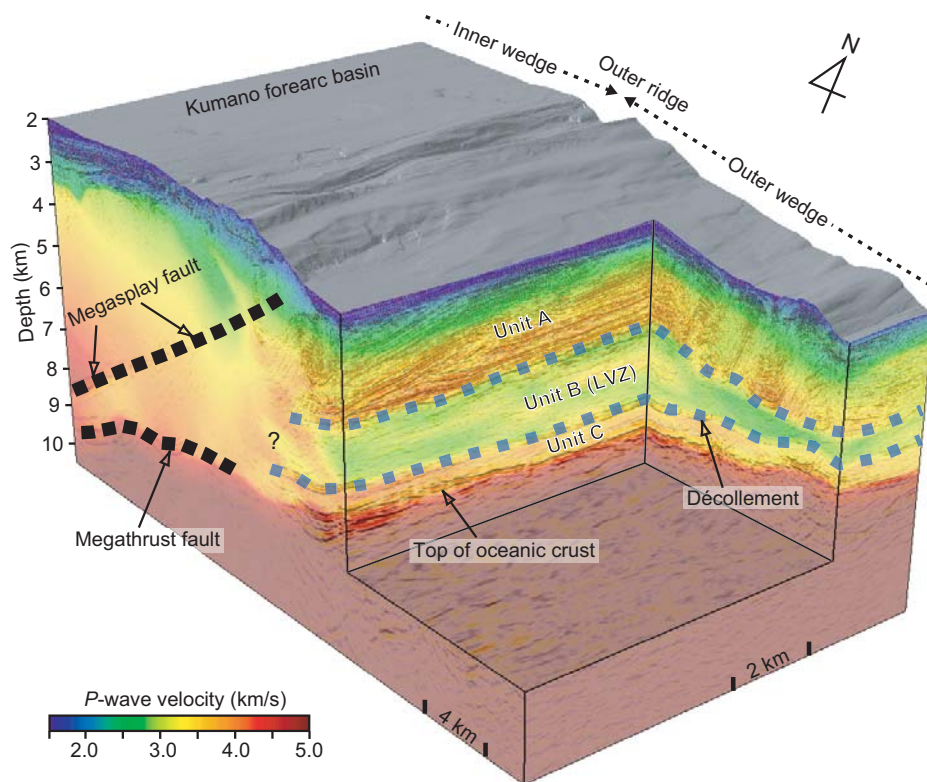


**Figure 3.** Three-dimensional view (3-D) of seismic reflection image overlain by  $P$ -wave velocity (in color) from 3-D prestack depth migration (PSDM) and interpretation of low-velocity zone (LVZ). Light blue thick and dotted area marks LVZ (unit B) in outer wedge. Extension of LVZ toward inner wedge is not obvious.

<sup>1</sup>Figures 2, 4, and 5 are provided as a separate loose insert.

related to subducted and metamorphosed sediments. Another LVZ with high reflectivity in the Chile margin (Groß et al., 2008) may represent the fluid-filled subduction channel. The nature and origin of the weak reflectivity of the LVZ along the Nankai wedge are not yet clear. We note a similar, weak reflectivity of unit B (LVZ) and unit C, suggesting a small lithology contrast between the two nearby units. Assuming that unit B originated from the underthrusting unit C, consisting of homogeneous, hemipelagic muddy sediments, unit B may simply exhibit weak reflectivity. Considering that the reflectivity is produced from acoustic impedance (velocity  $\times$  density), the weak reflectivity may be indicative of a small density contrast within the fluid-filled LVZ materials.

### Wide-Angle OBS Data and the LVZ Distribution

Wide-angle OBS data (Fig. 4; see footnote 1) support the lower velocity of unit B. Several OBSs around the LVZ (unit B) of the outer wedge recorded a shadow zone, or a significant decline of first arrival amplitude. For example, we clearly identify the shadow zone between offsets 13 km and 19 km in the OBS97 data (Fig. 4A). Comparing the observed wide-angle seismic data of OBS97 (Fig. 4A) with synthetic ray-paths of first arrivals calculated on inline 2535 (Fig. 4B), the shadow zone is closely related to the diffracted rays from the bottom of unit A, caused by the velocity reversal between units A and B. This indicates that the LVZ is responsible for the shadow zone. Similar shadow zones are observed in other OBS data (Figs. 4C and 4D), suggesting a broad distribution of the LVZ along the Nankai subduction zone off the southeastern Kii Peninsula.

In order to map the lateral extent of the LVZ along the Nankai Trough margin, we examined many 2-D seismic reflection lines (Fig. 1) that have been acquired since the 1990s. Taking the weak reflectivity character as a primary key to identify the LVZ that is clearly recognized in the 3-D data allows us to determine the LVZ distribution along the Nankai Trough margin, even though its lower velocity controls are not obvious. Moreover, several OBSs showing the shadow zone help to constrain the distribution of the LVZ. Based on these MCS and OBS data, we infer that the LVZ is predominant along the outer accretionary wedge between the frontal thrust and outer ridge off the Kumano forearc basin (Fig. 1). The LVZ is estimated to be a maximum of  $\sim 2$  km thick,  $\sim 15$  km wide, and  $\sim 120$  km long.

### TECTONIC EVOLUTION AND IMPLICATIONS OF THE LVZ

The discovery of the LVZ provides new insights into the structure and processes in the

Nankai subduction zone. Interpretation of the formation of the LVZ is somewhat controversial. One of the simple interpretations is that the LVZ could be an underthrust package underplated in response to the lateral growth of the accretionary prism. Davis et al. (1983) demonstrated that the accretionary prism will maintain a critical taper in response to the forces acting upon the subduction system. We propose an underplating-related tectonic model for the formation of the LVZ (Fig. 5; see footnote 1). Units A and C would represent a preexisting accretionary prism and underthrust sediments, respectively (Fig. 5A). Underplating of unit C beneath unit A would maintain a critical taper of the accretionary prism so that unit A can continue to grow seaward (Fig. 5B), thus being responsible for the formation of unit B. Antiformal stacking of thrust sheets (e.g., Twiss and Moores, 1992), consisting of sequences of underplated Shikoku Basin sediments, might produce a locally thicker LVZ with a maximum thickness of  $\sim 2$  km (Fig. 3). Similar underplating process accompanying the antiformal stacking was reported in the Alaska margin (Moore et al., 1991). Hyndman and Wang (1993) proposed that the dehydration due to conversion of stable-sliding smectite to stick-slip illite was almost complete at temperatures between 100 and 150 °C. In fact, the LVZ corresponds to an area of temperature  $>100$  °C (Kimura et al., 2007). Fluids coming from consolidation and clay mineral dehydration (e.g., smectite to illite transformation) of the underplated sediments (e.g., Moore and Vrolijk, 1992) may cause the seismic velocity to be lower than that of the overlying wedge.

Tanioka and Seno (2001) proposed that additional uplift of the sediments near the trench with a large horizontal movement due to megathrust earthquakes may have a large effect on tsunami generation. A study on Coulomb wedge theory (Wang and Hu, 2006) demonstrated that during megathrust earthquakes, the outer accretionary wedge is pushed into a compressively critical state, with an increase in basal and internal stresses. Assuming that a low seismic velocity along a shallow subduction zone is generally related to a high fluid content (e.g., Sage et al., 2006), the LVZ along the Nankai wedge should be in a condition of high fluid pressure, which is more likely to reduce the rigidity (the resistance to shear deformation) of the entire outer accretionary wedge. We speculate that the rigidity-lowered outer wedge, containing the LVZ, may undergo more easily the additional uplift due to a coseismic horizontal movement of the backstop, and thus eventually foster tsunami generation. A tsunami waveform inversion study (Baba and Cummins, 2005) indicated that the 1944 Tonankai (*M* 8.1) coseismic rupture off the southeastern Kii Peninsula propagated anomalously

seaward beyond the outer ridge, unlike the 1946 Nankai (*M* 8.3) coseismic rupture off Shikoku Island. A megasplay fault system (Park et al., 2002; Moore et al., 2007) as shown in Figure 3, which is recognized as a first-order feature in the Nankai Trough margin off the southeastern Kii Peninsula, has been adopted to explain the different rupture pattern between those two events. The  $\sim 120$ -km-long LVZ, which is not identified off Shikoku Island, could be another structural factor for the different rupture pattern, in addition to the megasplay fault. For the 1944 Tonankai event, the coseismic rupture area estimated from tsunami waveform inversion (Tanioka and Satake, 2001) extends more seaward, compared with the coseismic area estimated from seismic waveform inversion (Kikuchi and Yamanaka, 2001). If we accept the resolution of those tsunami and seismic waveform inversions, the discrepancy between the two inversions may be caused by the tsunami due to the additional uplift of the outer wedge with the LVZ.

The geometry of the zone between the megasplay fault and the LVZ (Fig. 3) suggests that the LVZ will join the footwall of the fault as the Philippine Sea plate subducts deeper. When the fluid-rich LVZ meets the megasplay fault, it may supply a significant amount of the fluid to the fault zone (Bangs et al., 2009). Stick-slip behavior in a fault zone requires that the strength should be recovered after any slip event, so that the earthquake failure can repeat (Moore and Saffer, 2001). Enhanced mineral precipitation caused by active migration of the fluid could contribute to the healing of the megasplay fault. Accordingly, the megasplay fault, being a weak fault zone, is likely to be repeatedly chosen as an easy pathway for rupture propagation of the Nankai earthquakes.

### ACKNOWLEDGMENTS

We thank Y. Kido, S. Sato, S. Uraki, T. Tsuji, Y. Sanada, A. Nakanishi, G. Kimura, and Y. Kaneda for their help in seismic data processing and interpretation. We also thank Casey Moore, Boris Marcaillou, and an anonymous reviewer for their helpful comments and suggestions. We also thank *Geology* editor Sandra Wyld. This research was supported by the Japanese Ministry of Education, Culture, Sports and Technology (MEXT) and the U.S. National Science Foundation (NSF).

### REFERENCES CITED

- Ando, M., 1975, Source mechanisms and tectonic significance of historical earthquakes along the Nankai trough: *Tectonophysics*, v. 27, p. 119–140, doi: 10.1016/0040-1951(75)90102-X.
- Baba, T., and Cummins, P.R., 2005, Contiguous rupture areas of two Nankai Trough earthquakes revealed by high-resolution tsunami waveform inversion: *Geophysical Research Letters*, v. 32, L08305, doi: 10.1029/2004GL022320.
- Bangs, N.L.B., Moore, G.F., Gulick, S.P.S., Pangborn, E.M., Tobin, H.J., Kuramoto, S., and Taira, A., 2009, Broad, weak regions of the Nankai megathrust and implications for shallow coseismic slip: *Earth and Planetary Science*

- Letters, v. 284, p. 44–49, doi: 10.1016/j.epsl.2009.04.026.
- Christeson, G.L., McIntosh, K.D., Shipley, T.H., Flueh, E., and Goedde, H., 1999, Structure of the Costa Rica convergent margin, offshore Nicoya peninsula: *Journal of Geophysical Research*, v. 104, p. 25,443–25,468.
- Davis, D., Suppe, J., and Dahlen, F.A., 1983, Mechanics of fold-and-thrust belts and accretionary wedges: *Journal of Geophysical Research*, v. 88, p. 1153–1172.
- Groß, K., Micksch, U., and TIPTEQ Research Group, Seismics Team, 2008, The reflection seismic survey of project TIPTEQ—The inventory of the Chilean subduction zone at 38.2°S: *Geophysical Journal International*, v. 172, p. 565–571, doi: 10.1111/j.1365-246X.2007.03680.x.
- Hyndman, R.D., and Wang, K., 1993, Thermal constraints on the zone of major thrust earthquakes failure: The Cascadia subduction zone: *Journal of Geophysical Research*, v. 98, p. 2039–2060, doi: 10.1029/92JB02279.
- Ishibashi, K., 1983, Tectonic significance of the 1605 Keicho tsunami earthquake off Tokai-Nankai, Japan: *Seismological Society of Japan Abstracts*, v. 1, p. 96.
- Kikuchi, M., and Yamanaka, Y., 2001, Rupture process of great earthquakes: Identification of asperity: *Seismo*, v. 7, p. 6–7.
- Kimura, G., and Mukai, A., 1991, Underplated units in an accretionary complex: Melange of the Shimanto Belt of eastern Shikoku, southwest Japan: *Tectonics*, v. 10, p. 31–50.
- Kimura, G., Kitamura, Y., Hashimoto, Y., Yamaguchi, A., Shibata, T., Ujiie, K., and Okamoto, S., 2007, Transition of accretionary wedge structures around the up-dip limit of the seismogenic subduction zone: *Earth and Planetary Science Letters*, v. 255, p. 471–484, doi: 10.1016/j.epsl.2007.01.005.
- Kosloff, D., Sherwood, J., Koren, Z., Mchet, E., and Falkovitz, Y., 1996, Velocity and interface depth determination by tomography of depth migrated gathers: *Geophysics*, v. 61, p. 1511–1523, doi: 10.1190/1.1444076.
- Moore, G.F., Shipley, T.H., Stoffa, P.L., Karig, D.E., Taira, A., Kuramoto, S., Tokuyama, H., and Suyehiro, K., 1990, Structure of the Nankai Trough accretionary zone from multichannel seismic reflection data: *Journal of Geophysical Research*, v. 95, p. 8753–8765, doi: 10.1029/JB095iB06p08753.
- Moore, G.F., Bangs, N.L., Taira, A., Kuramoto, S., Pangborn, E., and Tobin, H.J., 2007, Three-dimensional splay fault geometry and implications for tsunami generation: *Science*, v. 318, p. 1128–1131, doi: 10.1126/science.1147195.
- Moore, G.F., and 14 others, 2009, Structural and seismic stratigraphic framework of the Nankai TroSEIZE Stage 1 transect, in Kinoshita, M., et al., *Proceedings of the IODP, 314/315/316: College Station, Texas, Integrated Ocean Drilling Program Management International, Inc.*, doi: 10.2204/iodp.proc.314315316.102.2009.
- Moore, J.C., and Saffer, D., 2001, Updip limit of the seismogenic zone beneath the accretionary prism of southwest Japan: An effect of diagenetic to low-grade metamorphic processes and increasing effective stress: *Geology*, v. 29, p. 183–196, doi: 10.1130/0091-7613(2001)029<0183:ULO TSZ>2.0.CO;2.
- Moore, J.C., and Silver, E.A., 1987, Continental margin tectonics: Submarine accretionary prisms: *Reviews of Geophysics*, v. 25, p. 1305–1312.
- Moore, J.C., and Vrolijk, P., 1992, Fluids in accretionary prisms: *Reviews of Geophysics*, v. 30, p. 113–135.
- Moore, J.C., Diebold, J.B., Fisher, M.A., Sample, J.C., Brocher, T.M., Talwani, M., Ewing, J.I., von Huene, R., Rowe, C., Stone, D., Stevens, C., and Sawyer, D.S., 1991, EDGE deep seismic reflection transect of the eastern Aleutian arc-trench layered lower crust reveals underplating and continental growth: *Geology*, v. 19, p. 420–424, doi: 10.1130/0091-7613(1991)019<0420:EDSRTO>2.3.CO;2.
- Nakanishi, A., Kodaira, S., Miura, S., Ito, A., Sato, T., Park, J.-O., Kido, Y., and Kaneda, Y., 2008, Detailed structural image around splay fault branching in the Nankai subduction seismogenic zone: Results from a high-density ocean-bottom seismic survey: *Journal of Geophysical Research*, v. 113, B03105, doi: 10.1029/2007JB004974.
- Nedimovic, M.R., Hyndman, R.D., Ramachandran, K., and Spence, G.D., 2003, Reflection signature of seismic and aseismic slip on the northern Cascadia subduction interface: *Nature*, v. 424, p. 416–420.
- Okino, K., Shimakawa, Y., and Nagaoka, S., 1994, Evolution of the Shikoku Basin: *Journal of Geomagnetism and Geoelectricity*, v. 46, p. 463–479.
- Park, J.-O., Tsuru, T., Kaneda, Y., Kono, Y., Kodaira, S., Takahashi, N., and Kinoshita, H., 1999, A subducting seamount beneath the Nankai accretionary prism off Shikoku, southwestern Japan: *Geophysical Research Letters*, v. 26, p. 931–934.
- Park, J.-O., Tsuru, T., Kodaira, S., Cummins, P.R., and Kaneda, Y., 2002, Splay fault branching along the Nankai subduction zone: *Science*, v. 297, p. 1157–1160, doi: 10.1126/science.1074111.
- Park, J.-O., Moore, G.F., Tsuru, T., Kodaira, S., and Kaneda, Y., 2003, A subducted oceanic ridge influencing the Nankai megathrust earthquake rupture: *Earth and Planetary Science Letters*, v. 217, p. 77–84, doi: 10.1016/S0012-821X(03)00553-3.
- Sage, F., Collot, J.-Y., and Ranero, C.R., 2006, Interplate patchiness and subduction-erosion mechanisms: Evidence from depth-migrated seismic images at the central Ecuador convergent margin: *Geology*, v. 34, p. 997–1000, doi: 10.1130/G22790A.1.
- Seno, T., Stein, S., and Gripp, A.E., 1993, A model for the motion of the Philippine Sea plate consistent with NUVEL-1 and geological data: *Journal of Geophysical Research*, v. 98, p. 17,941–17,948, doi: 10.1029/93JB00782.
- Stork, C., 1992, Reflection tomography in the post-migrated domain: *Geophysics*, v. 57, p. 680–692, doi: 10.1190/1.1443282.
- Tanioka, Y., and Satake, K., 2001, Detailed coseismic slip distribution of the 1944 Tonankai earthquake estimated from tsunami waveforms: *Geophysical Research Letters*, v. 28, p. 1075–1078, doi: 10.1029/2000GL012284.
- Tanioka, Y., and Seno, T., 2001, Sediment effect on tsunami generation of the 1896 Sanriku tsunami earthquake: *Geophysical Research Letters*, v. 28, p. 3389–3392, doi: 10.1029/2001GL013149.
- Twiss, R.J., and Moores, E.M., 1992, *Structural geology*: New York, W.H. Freeman and Company, 532 p.
- Wang, K., and Hu, Y., 2006, Accretionary prisms in subduction earthquake cycles: The theory of dynamic Coulomb wedge: *Journal of Geophysical Research*, v. 111, B06410, doi: 10.1029/2005JB004094.
- Yilmaz, Ö., 2001, *Seismic data analysis processing, inversion and interpretation of seismic data*: Tulsa, Oklahoma, Society of Exploration Geophysicists, 2027 p.

Manuscript received 9 March 2009

Revised manuscript received 6 October 2009

Manuscript accepted 7 October 2009

Printed in USA

## ERRATUM

### Taking mylonites' temperatures

M.J. Kohn and C.J. Northrup

*(Geology*, Vol. 37, No. 1, p. 47–50)

At the prompting of M. Stipp, we realized that one of the strain calculations in Kohn and Northrup (2009) could not be reconciled with our reported grain sizes. Whereas a grain size of 7  $\mu\text{m}$  for sample CC8-3-2 does yield a differential stress of  $\sim 140$  MPa, the calculated strain rate should be  $\sim 1 \times 10^{-10} \text{ s}^{-1}$ . Dr. Stipp

also correctly questioned our assumed water fugacity. Whereas the value of 400 MPa was chosen to be illustrative, realistic values would be approximately  $40 \pm 10$  MPa for CC6-9-2, and  $100 \pm 25$  MPa for CC8-3-2. These values imply strain rates of  $\sim 1 \times 10^{-16} \text{ s}^{-1}$  for CC6-9-2 (rather than  $3 \times 10^{-16} \text{ s}^{-1}$  as published), and  $\sim 3 \times 10^{-11} \text{ s}^{-1}$  for CC8-3-2 (fortuitously the same as published).

These changes do not affect the principal conclusions of the study, namely that some quartz

mylonites appear to reequilibrate with respect to Ti content, that the Ti-in-quartz thermometer (Wark and Watson, 2006) can be used to estimate temperatures of mylonitization, and that different textures in mylonites can reflect orders of magnitude differences in strain rate, rather than temperature.

Wark, D. A., and Watson, E. B., 2006, TitaniQ: A titanium-in-quartz geothermometer: *Contributions to Mineralogy and Petrology*, v. 152, p. 743–754.

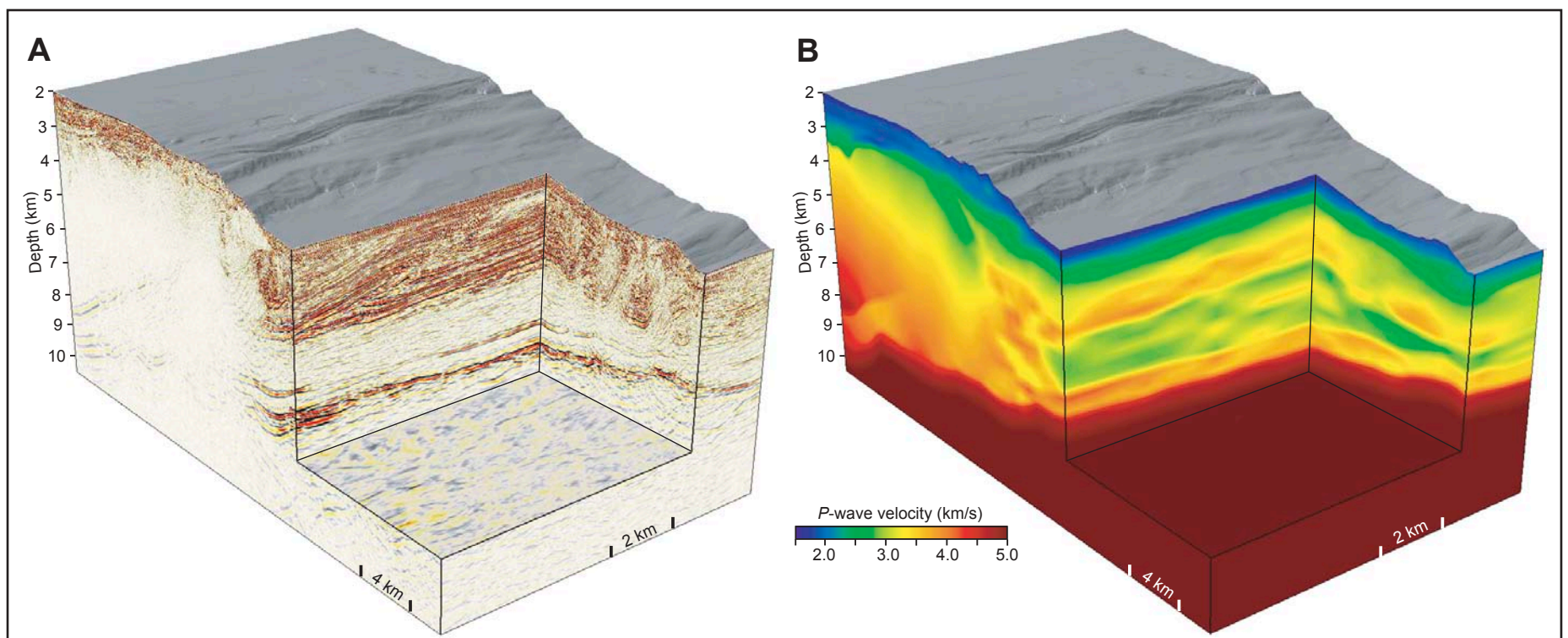


Figure 2. Final 3-D prestack depth migration (PSDM) results. A: 3-D view of seismic reflection image. B: *P*-wave velocity model derived from the 3-D PSDM. We used a commercial seismic vessel, *M/V Nordic Explorer* of Petroleum Geo-Services (PGS), for the 3-D survey. As the sound source, we deployed two arrays, each with 28 G-guns totalling 51 L (3090 in<sup>3</sup>), fired alternately at 37.5 m shot interval. The 3-D survey used four receiver cables spaced 150 m apart, each 4500 m long with 360 receiver groups at 12.5 m spacing. This 4-streamer/2-source array geometry yielded eight source-receiver common midpoint (CMP) lines per sail line at a spacing of 37.5 m and nominal 30

fold data. The 3-D data set was processed through 3-D prestack time migration (PSTM) by Compagnie Générale de Géophysique (CGG). After applying noise attenuation, multiple suppression, amplitude correction, and trace interpolation, the 3-D data were sorted into 12.5 m × 18.75 m CMP bins (Moore et al., 2009). Using the CMP bin gathers preconditioned by CGG, we performed migration velocity analysis for the 3-D PSDM at Japan Agency for Marine Earth Science and Technology (JAMSTEC). We created a 3-D initial RMS velocity model using RMS vertical velocities, and then updated the 3-D RMS velocity model by several iterations of both 3-D prestack time migration and residual RMS velocity analysis (Yilmaz, 2001). After converting the 3-D RMS velocity model to the 3-D initial interval velocity model using the Dix formula, we updated the 3-D interval velocity model by several iterations of both 3-D PSDM and 3-D horizon-based tomography (Kosloff, 1996). For the final refinement of the 3-D interval velocity model, we applied 3-D grid-based tomography (Stork, 1992), and then applied full 3-D Kirchhoff PSDM with aperture size of 6 km × 8 km. Ocean bottom seismograph (OBS) velocity data (Nakanishi et al., 2008) on a wide-angle seismic line that passes through the 3-D survey box guided the 3-D PSDM velocity model building.

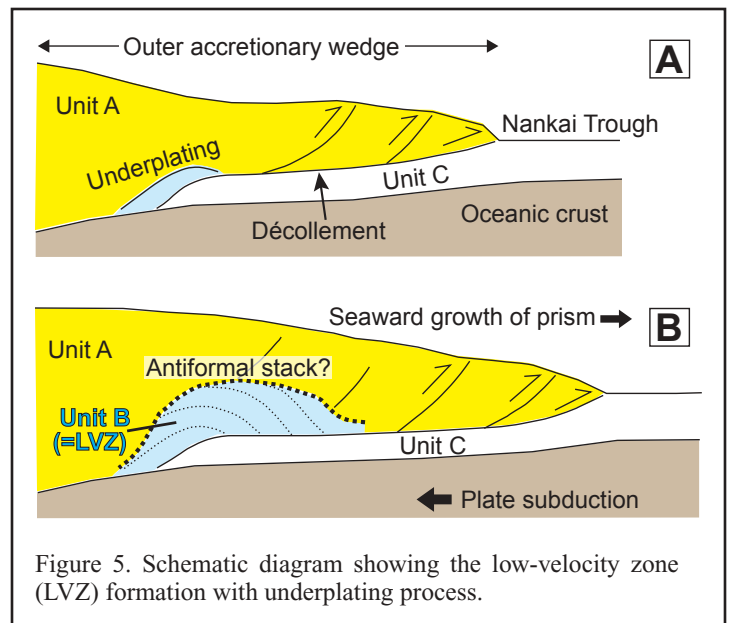
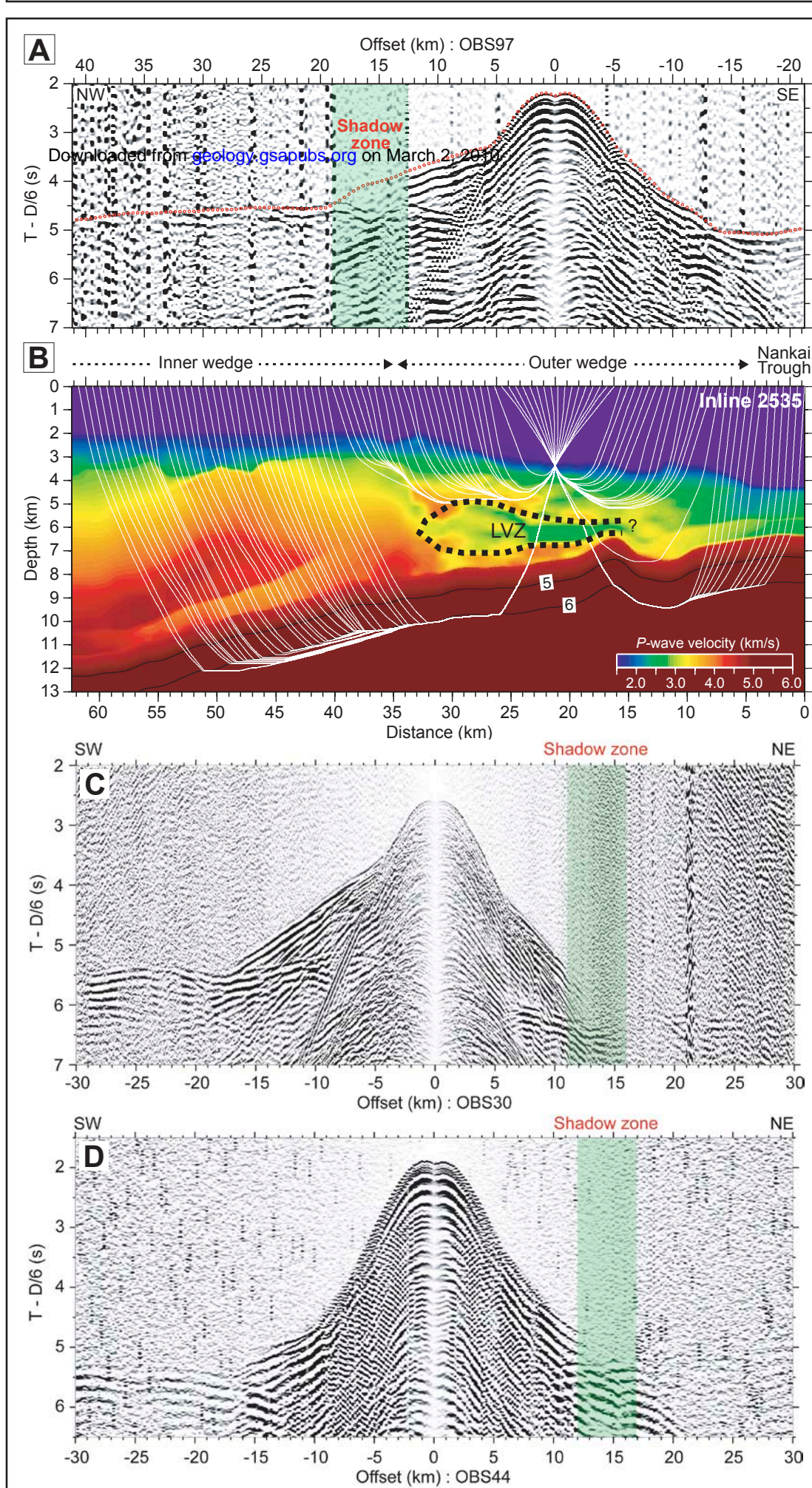


Figure 5. Schematic diagram showing the low-velocity zone (LVZ) formation with underplating process.

Figure 4. Wide-angle ocean bottom seismograph (OBS) records showing the shadow zone. A: Observed wide-angle seismic data from OBS97 on inline 2535 of 3-D survey area. The vertical axis is reduced by 6 km/s. The horizontal axis indicates offset distance from the OBS. Red dots mark travel times of the first arrival refractions, which are calculated on the basis of the 3-D prestack depth migration (PSDM)-derived velocity model along inline 2535. These synthetic travel times of the first arrivals are in excellent agreement with OBS observations, indicating that the 3-D PSDM-derived velocity model is highly reliable. Note weak amplitude of the first arrivals between offset 13 km and 19 km, termed the shadow zone (in light green). B: 3-D PSDM-derived velocity model along inline 2535 and synthetic ray-paths (white thin lines) of first arrivals calculated on inline 2535. In the outer wedge, the LVZ is marked in black dotted line. C: Observed wide-angle seismic data from OBS30. Note weak amplitudes of the first arrivals between offsets 11 km and 16 km, termed the shadow zone (in light green). D: Observed wide-angle seismic data from OBS44. We observe weak amplitudes of the first arrivals between offsets 12 km and 17 km, termed the shadow zone (in light green). Shot spacing for all the OBS data is 200 m (Nakanishi et al., 2008).